Paddy and Water Environment, DOI: 10.1007/s10333-013-0371-5.

Measurement of soil salinity using electromagnetic induction in a paddy with a densic pan and shallow water table

Juan Herrero • Wayne H. Hudnall

Juan Herrero

Estación Experimental de Aula Dei, CSIC, PO Box 13034, 50080 Zaragoza, Spain

e-mail: jhi@eead.csic.es; phone + 34 976 716 152, fax 34 976 716 145

Wayne H. Hudnall (deceased)

Department of Plant and Soil Science, Texas Tech University, Lubbock, TX 79409, USA

Abstract Rice (*Oryza sativa* L.) has become a monoculture in the saline lands of the Ebro Valley, Spain. The studied farm has produced rice since the 1970s; one exception was 1999, which enabled us to map the soil salinity. The farm had lateral salinity variations mirrored by the development of rye grass (*Lolium multiflorum* Lam.) planted in 1999. Our objective is to prove the value of a non-deterministic method using electromagnetic induction (EMI) to map the salinity of the rootable layer in the unfavorable circumstances of a paddy having shallow saline and quasi-artesian water table underneath a continuous densic layer. From our EMI readings and soil sampling, we draw a map of the electrical conductivity of saturated paste extracts (ECe) of the upper soil layer (0-40 cm), with ECe ranging from 1.6 dS m^{-1} to 20.8 dS m^{-1} and a mean of 7.9 dS m^{-1}. A main achievement was the establishment of an easy procedure not requiring either: (i) knowledge regarding the salinity of the water table or the relationships between EMI readings and the deep soil composition; or (ii) a normal distribution of the EMI readings or of the ECe; or (iii) assumptions about the physical dimensions of the EMI readings. Our procedure will allow ECe to be mapped on other similar salt-affected paddies, helping to decide if a paddy can be planted with alternate crops for production, weed control, or soil structure improvement.

Key words: Irrigation • Paddy soil • Rice • Spain

Introduction

Puddled rice is a sound productive choice for agriculture in saline Mediterranean inland areas where irrigation water of low electrical conductivity is available. This is the case for the Flumen irrigation district (Nogués et al. 2000), located in the semiarid Central Ebro Valley, NE Spain, where rice has been grown for about 60 years as the only economically feasible crop due to soil salinity, even though rice is not a highly salt-tolerant crop. As long as the soil is puddled and the paddy is flooded, the high-quality irrigation water prevents the saline groundwater underneath the puddle zone from contaminating the paddy rice rooting zone. The soil is puddled using the fallow straw to develop a compact soil pan at about 40 cm depth, which is comparable to a continuous adobe layer. This impervious densic pan prevents rice roots penetration, decreases infiltration and impedes the rise of saline water. Rice yields are economically satisfactory because the rice plants depend only on the soil layer overlying the pan and on the water (about 2000 mm yr^{-1}) required in this area to maintain rice under continuously flowing water with a depth of about 10 cm (Playán et al. 2008).

The oldest and most typical paddies in Flumen are located within the landscape depressions. Shallow, saline water tables are common in these depressions because of paddy rice from May 1st to September, and because the upper conterminous lands are irrigated producing subsurface flow into the depressions through the saliferous strata. Most paddies remain waterlogged or muddy throughout the year. Moreover, the subsurface soil is oversaturated. In most years, these conditions hinder soil sampling with commonly available tools, as well as the use of field techniques based upon the electrical or the electromagnetic properties of the soil.

Because of these reasons, there is essentially no salinity data for the root-usable soil volume by rice or by rotationary crops. Electromagnetic induction (EMI) measurements and limited strategically located field data could produce both maps and average salinity values for this layer if it were not flooded and/or saturated. For interpretation in agricultural systems, the EMI readings must be converted to a standard measure of soil salinity, such as the electrical conductivity of the saturation extract (ECe).

Researchers have used EMI to map soil salinity within plots around the world, as reviewed by Rhoades et al. (1999) and also for Flumen and other irrigation districts in the Ebro Valley (Amezketa 2006). The soil depth investigated was about 1 m in most cases, but EMI data also have been correlated with soil salinity at other depths in the Flumen district (Herrero et al. 2003; Nogués et al. 2006; Playán et al. 2008; Herrero et al. 2011). However, the permanence of a saline water table under the densic pan in the old paddies of Flumen's irrigated districts raised the question whether EMI would be applicable for salinity assessment of the rooting layer above the densic pan. Under supersaturated or flooded conditions soil salinity cannot be measured by the classical sampling methods. Moreover, rice development does not mirror these saline differences provided it is cultivated as a paddy with flowing fresh water.

Most salinity problems in paddies occur in river deltas or other coastal areas, and are caused by seawater intrusion or low-quality irrigation water; however, few studies have used EMI to measure the soil salinity of paddies (Enrique et al. 2005; Li et al. 2013); rather, most EMI surveys in paddy plots have been conducted on non-saline soils in humid areas (Aimrun et al. 2007, 2011; Ezrin et al. 2010; Islam et al. 2011) for purposes other than soil salinity mapping. To our knowledge, no published studies have used EMI to measure agricultural salinity in the unfavorable conditions of a paddy that is underlain by a shallow saline water table.

One of the most popular EMI instruments is the EM38 sensor (Geonics Ltd., Mississauga, Ontario, Canada). EM38 is easily hand-held because it weighs only about 3.6 kg and is only 1.05 m long (Fig. 1). EM38 is based on two parallel coils at a fixed distance of 1 m (Fig. 1 a). A primary magnetic field created by the emitter coil induces small currents in conductor materials such as the soil. The secondary magnetic field created by these currents, superimposed on the primary magnetic field, excites the receiver coil with an intensity that is read on a dial. The intensity often differs according to whether the sensor is placed with its coils vertical (Fig. 1b) or horizontal (Fig. 1c), due to the different pattern of contribution to the signal made by the successive soil layers, with a greater relative contribution from shallow layers if the coils are horizontal (Rhoades et al. 1999). These contribution patterns and other details of the EMI response have been discussed in McNeill (1980) and in López-Bruna and

Herrero (1996). According to these authors, the physical dimensionality of the signal, and thus its units, can be controversial. This matter is overcome by adopting an empirical method without assigning units to the EMI readings. Our approach to converting the EMI readings into ECe estimations is statistical, and not deterministic; i.e., it relies on targeted sampling strategies and regression calibrations, as described by Lesch et al. (2005**).**

The literature provides few examples of the use of EM38 for salinity assessment in paddies with conditions similar to Flumen, where the EMI signal is influenced by the non-targeted saline and supersaturated deep layers. EM38 has been used by Li et al. (2013) for generating a three-dimensional model of soil salinity in a paddy including the deep soil. In the present article we avoid to consider the relative contribution of the non-targeted deep layers to the EM readings. We mapped the soil salinity of a target layer (0-40 cm) in a saline paddy using the classical calibration of EMI readings with ECe measured in a few soil samples. The objective was to simplify the soil salinity mapping in puddled soils by testing that assumptions about (i) the composition of the oversaturated saline layer below the densic pan, (ii) the normality of the regressed data, and (iii) the physical dimension of the EMI readings, are unnecessary. The mapping has practical implications for agricultural management.

Materials and methods

The studied farm is located in the Ebro Valley, NE Spain (Fig. 2), municipality of Almuniente. The area was intensively leveled for basin and border irrigation in the 1950's. The climate is semiarid, with mean annual temperature of 15.3ºC, 434 mm precipitation, and 1188 mm reference evapotranspiration (ET_0), according to the records of the Almuniente weather station, located 2 km from the farm. The parent material for the soils is Quaternary deposits of alternating millimetric layers of silt and sodic clay from Miocene saliferous strata that outcrop along the surrounding slopes. Soils are saline or saline-sodic, with weak structure, and are classified as Oxyaquic Xerofluvents (Soil Survey Staff 2010).

The farm, with an area of 14 ha, is divided into 7 plots as shown by the aerial photograph of Fig. 3. Plots are in steps descending from plot 1 to plot 7, and with a berm between them.

117 Irrigation water is distributed to each plot by individual gates in an elevated irrigation ditch
118 built in concrete. Table 1 shows composition data for a soil profile described in July 1979 at
119 plot no. 1 plus the ECe for synthetic layers of 20 cm depth calculated with the method of
120 Herrero and Pérez-Coveta (2005) by averaging ECe with data from six cores taken at two sites
121 of plot no.1 in 1979-1980, and by averaging the data from six cores taken in 1999-2000 at the
122 same sites. The ECe of the upper meter of the soil in plot no. 1 ranged from 40 to 45 dS m^{-1},
123 and sodium adsorption ratio (SAR) from 85 to 100 in 1979-80. In 1999-2000, the ECe was 2
124 dS m^{-1} and SAR was about 2 (Herrero 2008). This noticeable decrease can be attributed to the
125 continuous flooding of the paddies with fresh, running irrigation water. A saline water table
126 with an electrical conductivity ranging from 0.95 to 4.87 dS m^{-1} (mean 2.28 dS m^{-1}), was
127 measured during February and August, 1999. This range of salinity is common during the
128 irrigation season. The soil surface was wet and often ponded for most of the field visits during
129 1999-2000. After stopping the flooding to allow the harvest of rice, in September 1999, the
130 entire farm was planted with Promenade Italian rye grass (*Lolium multiflorum* Lam., var.
131 Westerwoldicum). In November, it was less than 15 cm tall in many areas of the farm. Rye
132 grass planted in plots no. 3 to 6 had irregular cover, with spots where the seed did not
133 germinate. The circumstance of having a non-flooded crop provided an opportunity to map the
134 root zone soil salinity.

135 EMI readings were performed with a hand-held EM38 sensor. The EMI readings and soil
136 sampling were conducted from orthogonal grids. After marking the grid points with stakes,
137 EM38 readings were obtained from these sites a few days after irrigation. Soil temperature
138 was measured at 20 and 40 cm depth. At each site, the EM38 readings were taken with coils in
139 horizontal and in vertical position. After correcting for average temperature according to
140 Rhoades et al. (1999, page 6) to the standard temperature of 25ºC, and dividing by 100 to
141 simplify formulations, these EM38 readings were designated as EMh for horizontal coils and
142 as EMv for vertical coils. EMh and EMv give different information owing to their different
143 relative response vs. depth depending on the position of the coils (MacNeill 1980, Figure 6).
144 Table 2 summarizes the measurements with EM38.

On September 10, 1999, the lateral gradient of soil salinity on the entire farm was established by the first EMI survey covering about 14 ha at the nodes of an orthogonal grid of 50 m × 50 m, producing a total of 100 reading sites. On November 19, 1999, three, 6 cm diameter perforated vertical pipes were installed to a depth of 150 cm (Fig. 3) to measure the water table level. Two pipes, T1 and T2, were located within plot no. 2 at 0.5 m from the borders and 30 m and 180 m from the road, respectively. The third pipe, T3, was located within plot no. 1.

On December 15, 1999, 250 sites were located in the selected plot no. 2 (2.3 ha) at the nodes of an orthogonal 10 m × 10 m grid (Fig. 4), more dense at the corner where machinery wreck disturbed the EMI signal. After completing the EMI readings, 40 sites were chosen for further soil sampling up to 40 cm depth based on the following criteria: (i) to span the range of the EMI readings, and (ii) to accomplish approximately uniform coverage across plot no. 2.

Soil samples for gravimetric water content (θ) determination were transported to the lab in hermetically sealed cans and weighed the same day. Samples for salinity determination, transported in polyethylene bags, were air-dried and ground in a sieving mill with 2-mm mesh openings. All subsequent determinations were performed on the fine earth (< 2-mm fraction). Percent of saturation (PS) of the saturated paste and ECe reported in dS m^{-1} at 25ºC were determined for each sample (United States Salinity Laboratory Staff 1954), with PS used as a surrogate of textural composition. The major ions (Ca^{2+}, Mg^{2+}, Na^{+}, K^{+}, CO_3^{2-}, HCO_3^{-}, Cl^{-}, SO_4^{2-}) from six soil sites chosen at random (Fig. 4) were determined from the saturation extracts, and the SAR calculated; pH was measured on the same extract (pHe).

On April 19, 2000, the EMI readings were not consistent with the visual symptoms of salinity because the soil was too dry in some areas, i.e., outside the allowable range of soil moisture for EMI measurements of not less than about one-half of field-capacity water content (Rhoades et al. 1999). The rye grass showed maximum development within plot no. 2, but broad, bare surfaces showing salt efflorescence were noted.

EMh, EMv, and lab data were analyzed using histograms, centrality measures (mean, median, quartiles) and dispersion measures (variance, standard deviation, and coefficient of

variation). Normality was studied using the Kolmogorov-Smirnov test. Boxplots were drawn according to the conventions established by Chambers et al. (1983).

Relationships between EMh and EMv

For each of the two dates of calibration, EMh and EMv were examined and their relative magnitudes visualized by histograms, scatter diagrams, and boxplots. The regressions between EMh and EMv allowed the determination of colinearity between the horizontal and the vertical reading modes for several groupings of EMI data sets.

We tested two groupings by paralleling Rhoades et al. (1999) when they conducted separate calibrations of the EMI sensor depending on if the deep soil salinity is predominant ("regular profiles"), or not ("inverted profiles"). We used two arbitrary thresholds; the first was $EMv \geq EMh$, and the second $EMv \geq EMh + 0.1$ to obtain different batches of data for regressions. Maintaining our empirical approach, the purpose of our thresholds was not to investigate or to hypothesize about the vertical distribution of salinity, water content or other soil characteristics influencing the EMI readings. Notwithstanding, for sake of brevity we use the denominations "regular" and "inverted".

Regressions

ECe was regressed on EMh and EMv to estimate soil salinity from EMI readings of those sites without soil sampling. Independent calibrations of the EM38 with ECe were tested for the sites with high contribution to EMI response from the deep layers, using the two above mentioned thresholds.

The frequency distributions were not Gaussian, a very common case for soil salinity (Isaaks and Srivastava 1989). Box-Cox transformations (Myers 1990) were applied trying to obtain normality, without satisfactory results. Multiple linear regressions were applied to check the relationship of ECe with EMh and EMv. For the multiple regressions of ECe on

EMh and EMv, EMh and EMv were transformed to their natural logarithms. Colinearity between these two measurements was reduced by taking the difference between the natural logarithms of EMh and EMv as the second explanatory variable, instead of EMv (Lesch et al. 1992).

As the above methods did not improve the results of the linear regression, a nonparametric simple regression was performed using the Theil method (Daniel 1990; Glaister 2005), which estimates the slope coefficient and the intercept of a regression line. For a set of n pairs of observations (x_1, y_1), (x_2, y_2), . . ., (x_i, y_i), (x_j, y_j), . . ., (x_n, y_n) all of the data pairs are taken in order from small to large for the explanatory variable (x), from which are derived the slopes (B_{ij}) and the intercepts (A_{ij}) for each pair, i.e.:

$$B_{ij} = \frac{(y_j - y_i)}{(x_j - x_i)}; \quad where\ i < j \qquad \text{(Eq. 0)}$$

For each regression the $\binom{n}{2}$ values of B_{ij} are calculated as well as the same number of A_{ij}. The median of the B_{ij} values is taken as the slope of the straight-line regression and the median of (A_{ij}) as the intercept. In this study, the explanatory variable (x) is either EMh or EMv; the response variable (y) is ECe.

Lateral distribution of soil salinity

Both ECe determined in the lab and estimated from EMI readings were kriged using Surfer (Golden Software, Inc., Golden, CO) to obtain ECe contour lines. Study of the spatial statistics is beyond our scope, but these lines allowed examination of the soil salinity distribution across the plot. For the agricultural interpretation, we used the unequal soil salinity intervals previously applied in a nearby area (Nogués et al. 2006) of the irrigation district, based on Soil Survey Division Staff (1993).

Results and discussion

Salinity and hydrology settings

The EMh values from the 14 ha farm were used to draw contour lines at intervals of 0.25 EMh (Fig. 3). These contour lines of EMh can be indicators of soil salinity even before their conversion to ECe according to our previous experience in the Flumen district (Díaz and Herrero 1992; Lesch et al. 1992; Herrero et al. 2003; Playán et al. 2008) where linear relationships between ECe and EMh were found. The map showed that plot no. 2, with 2.3-ha extent, had the greatest variability of EMh among the plots, with an irregular growth of rye grass and bare spots.

This map showed differences in the salinity pattern of the plots, related to the earth movements needed to construct the leveled paddies no.1 to no. 7. Plot no. 1 is 0.4 m higher in elevation than plot no. 2. Ponding is more frequent in the areas with higher EMI readings. Comparing an aerial image with this map, there was a good match with the vegetation cover (Fig. 3).

When pipe T1 was installed in November 19, 1999, the water table was at 100 cm depth, but it rose to within 50 cm of the surface after two hours (Fig. 5). The water level at T2 was at 70 cm depth, and two hours later had risen to the soil surface. The water level remained constant at 70 cm depth at pipe T3. The water table is confined under the densic pan, as shown by the artesianism on November 20th. These observations illustrate the shallowness of the water table and its quasi-artesian condition at the time of the field studies.

Exploratory data analysis

Examination of EMh vs. EMv gives some insight into differences in the vertical distribution of soil features like salinity or moisture. EMh and EMv from the two dates, i.e., for the entire farm and for plot no. 2, cannot be collated due to the 96 days elapsed between them involving

254 changes in salts and water content in the soils. However, their distribution shapes and
255 measures of dispersion denote some differences between the whole farm and plot no. 2 (Fig.
256 6).
257
258 *EMI readings and salinity measures*
259
260 The frequency distributions of EMI readings for the farm (50 m × 50 m grid) and for plot no. 2
261 (10 m × 10 m grid) show similar skewness, but differ from the bimodal distributions of the
262 sampling sites. Bimodality also occurs within histograms of ECe.
263 For the 100 sites having EMI readings in the farm, both EMh and EMv have asymmetric
264 distributions tailing to the upper part, with EMv showing a broader range (Fig. 6). Values
265 greater than 2.25, considered high, are more frequent in EMv than in EMh, and the EMv
266 maximum is greater than the EMh maximum. The wider range and the other features of the
267 distribution of EMv compared with EMh can be related with the gradient of water and salt
268 content in the deep layers across the 800 m long farm. The different relationship for the 250
269 EMI reading sites at the plot scale may be due both to the smaller gradient and to the different
270 date of the readings.
271 For the 250 EMI reading sites from plot no. 2, EMh and EMv had similar ranges (Fig. 6)
272 with more than 60% of the values < 2.75. The distributions were asymmetric and tailed to the
273 upper part. EMh and EMv had high variability, with coefficients of variation (CV) of 45% and
274 39%, respectively. The many saline patches seen within the plot and the presence of an area
275 with no rye grass germination along the border with plot no. 1, support these CV's. The higher
276 CV for EMh can be attributed to a range of salinity or moisture in the plowed horizon greater
277 than in the densic pan or in the underneath saturated layers.
278 The distributions of EMh and EMv for the 40 augered sites were bimodal. These sites
279 were scattered all over the plot and through the range of salinity. This procedure did not
280 exactly preserve the distribution of the readings at the 250 sites in the plot, as shown by the
281 centrality measures of EMh and EMv higher at the 40 sampling sites than for the entire plot
282 no. 2 (Fig. 6), and by a greater interquartile range for the 40 sites.

283 The range of EMh and EMv for the 10 m × 10 m grid is higher than for the 50 m × 50 m
284 grid of plot no. 2 (Fig. 6), mainly because of the higher values recorded from the 10 m × 10 m
285 grid. Both features substantiate the variability of salinity, with saline areas not detected by the
286 50 m × 50 m grid.
287
288 *Soil moisture*
289
290 Gravimetric soil moisture (θ) determined at the lab on samples taken (0-40 cm) on December
291 15, 1999 ranged from 21% to 31%, with an average of 26%. These water contents are well
292 suited for calibrating the EM38 sensor to measure soil salinity (Rhoades et al. 1999). The
293 percent saturation (PS) of the saturated paste averaged 53%, ranging from 34% to 63%. This
294 large range shows the lateral variability of the texture of the upper soil layer within the studied
295 plot.
296 The regression of θ on PS obtained a low determination coefficient ($r^2 = 0.18$) and a non
297 significant slope ($p = 0.006$). This result substantiates that the moisture of the studied soil layer
298 at the time of sampling was not controlled by texture. The soil moisture on the date when plot
299 no. 2 was sampled was heterogenous. It could be attributed to subtle leveling irregularities
300 within the plot, provided the lateral variability in the deep soil is smaller than in the shallow
301 layers, as suggested by comparing the coefficient of variation of EMh (45%) versus EMv
302 (39%) in the 250 reading sites.
303 The correlation between θ and EMh, EMv, and ECe at the 40 sampling sites was very
304 weak, with non-significant correlation coefficients of 0.217, 0.174, and 0.218 ($p \geq 0.176$ for
305 the three cases), showing that θ did not influence the EMI readings or the ECe measured in the
306 lab. The results were similar for the groupings of EMh and EMv profiles according to the two
307 proposed thresholds.
308
309 *Analytical determinations*
310

311 Table 3 displays the analytical results for the analyzed samples ranked by their salinity. The
312 salinity range of these samples was high, as shown either by their ECe ranging from 2.96 to
313 20.80 dS m^{-1}, or by the content of the plant-stressing ions Mg^{2+}, Na^{+}, Cl^{-}, and SO_4^{2-}. The pHe
314 ranged from 7.97 to 8.18. Clays remain flocculated at these pH values and such high salt
315 content levels. The ranking of sites by salinity is the same as by SAR. Using soil salinity
316 classes listed by the Soil Survey Division Staff (1993, page 193), the mean ECe of these
317 samples (10.8 dS m^{-1}) qualifies as strongly saline, with all individual ECe greater than the 2 dS
318 m^{-1} threshold for slightly saline soils. Two samples surpassed the 16 dS m^{-1} threshold for very
319 strongly saline soils. Only two samples have SAR < 13; all the others are classified as sodic
320 (United States Salinity Laboratory Staff 1954). These two samples have by far the lowest ECe
321 and PS, illustrating the relationship of salinity and soil texture surrogated by PS.

322

323 *Relationships between EMh and EMv*

324

325 We maintain the widespread terms "regular/inverted profile" (Rhoades et al. 1999) for the
326 deep/shallow soil predominance of the EMI signal, even though the contribution of the
327 horizons is related to both water and salt content. The scatter plots of EMv and EMh are
328 presented in Fig. 7a and b for the 100 reading sites across the entire farm, in Fig. 7c and d for
329 the 250 reading sites in the plot no. 2. Crosses or circles in these figures stand for sites with a
330 regular or an inverted profile using two different thesholds: (i) sites where EMv ≥ EMh, and
331 (ii) sites where EMv ≥ EMh + 0.1. For the entire farm (Fig. 7a and b), regular profiles look
332 better adjusted to a straight line than all the 100 sites together. In contrast, the small number of
333 observations (circles in Fig. 7a) or the bimodal distribution (circles in Fig. 7b) of EMh and
334 EMv of the inverted profiles prevent the study of these relationships.

335 The direct comparison of readings at plot no. 2 with the 100 above-discussed readings is
336 impossible because of the different dates and areas of measurement. However, groups of
337 regular and inverted profiles show some similarities if Fig. 7c and d is compared with Fig. 7a
338 and b. The regular profile data fit better when adjusted to a straight line than the inverted

339 profiles do, even for the 250 sites (Fig. 7c and d), which have a non-bimodal distribution and
340 many more observations than Fig. 7a and b.

341 The considerations of the two above paragraphs apply better for the arbitrary threshold
342 EMv ≥ EMh + 0.1. The regressions of EMv on EMh were calculated separately for the 100
343 reading sites on the farm, the 250 reading sites from the plot, and the 40 sites with soil samples
344 (Table 4). Moreover, regressions were also calculated after splitting the sites according to the
345 two above criteria. A high coefficient of determination means a high colinearity of the two
346 readings. The second criterion (EMv ≥ EMh + 0.1) classified fewer sites as having high
347 contribution to the EMI readings from the deep layers. For the farm, i.e., 100 EMI reading
348 sites, only the second criterion allowed comparison of colinearity, but the difference was small
349 (r^2 = 0.97 versus r^2 = 0.99). For plot no. 2, i.e., 250 EMI reading sites, and their augered sites,
350 i.e., 40 EMI reading sites, these groupings show more colinearity for sites with a high
351 contribution from the deep layers, both for the plot and for the augered sites, and the stricter
352 the criterion the higher the colinearity.

353 The coherence of all parameters in Table 4 gives some credit even to those equations
354 with a low number of observations, and also supports the thesis that the 40 augering sites are
355 representative of plot no. 2. The colinearity for sites having EMv ≥ EMh, or EMv ≥ EMh + 0.1
356 can be related to water ponding at several of these sites, and with gravimetric water content >
357 28% for the upper horizon. The reason is that ponding could mask the high contribution to
358 EMI readings from deep layers supersaturated with saline water.

359 The equations obtained for the 250 reading sites and the 40 augered sites (Table 4), are
360 quite similar. The equations for sites with EMv ≥ EMh or with EMv ≥ EMh + 0.1 are almost
361 the same if either all the sites or only the augered ones are computed. The differences are
362 greater in the equations of shallow soil predominant probably because of the low number of
363 observations. These relationships support the representativity of the 40 sites.

364

365 Calibrations of EM38

366

The regressions of EMh and EMv on ECe (Table 5) convey the coherence of field measurements and lab determinations. The two last columns of this Table show the differences between least squares and Theil adjustments for both the intercept and the slope. The greater differences occur in Eq. 3, with only four samples and a non-significant slope ($p = 0.143$).

In spite of the colinearity between EMh and EMv discussed in the preceding section, Table 5 shows that the adjustments for EMh attain a higher r^2 and lower standard error (SE) than for EMv, i.e.: Eqs. 1, 2, 3, 4, and 5 vs. Eq. 6. The SE's of the EMh adjustments are smaller than for the EMv adjustment, except in Eq. 3, with only 4 effectives and with both intercept and slope non-significant.

The $r^2 = 0.86$ obtained by regressing ECe on EMh for all augered sites (Eq. 1) rises if only regular profiles according to either of the two considered thresholds are computed (Eqs. 2 and 4); SE's are also improved. The improvement in r^2 and SE obtained with the separate calibration for regular profiles after the first threshold (Eq. 2) seems promising. However, this result is not conclusive because the first threshold gives only 4 inverted profiles (Eq. 3, with no significant parameters), and the second threshold (Eq. 5) yields a worse adjustment for inverted profiles than Eq. 1. As expected, the adjustment with EMv (Eq. 6) is less satisfying than with EMh (Eq. 1). Strong (20%) decrease in r^2 in the predictions of ECe occurs when using EMv instead of EMh (Eq. 1 vs. Eq. 6). This can be attributed to the effect on the EMI signal produced by the supersaturated and saline horizon below 40 cm, with much more relative contribution to EMv than to EMh.

The multiple linear regressions of the direct salinity measures, ECe, on EMh and EMv, give coefficients significant at $p < 0.001$ only for EMh, as expected from the simple linear regression equations discussed in the above paragraph. The improvements of r^2 and SE against simple linear regression are slight. For ECe, the improvements of 0.8% in r^2 and 0.03 dS m^{-1} in the SE are well under the improvements of 4% for r^2 and 0.36 dS m^{-1} for SE obtained for regular profiles using the first threshold (Table 5, Eq. 2). The multiple linear regressions with the log transformed variables EMh and EMv did not obtain better results.

The calibration by the least squares regression obtain equations similar to Theil method, but this distribution-free method is preferred because Box-Cox transformations, logarithmic

396 transformations, or multiple linear regressions either did not meet the statistical requirements
397 for variables' distribution, or obtained not better adjustments than Theil method.

398 The last two columns of Table 5 show the differences between the intercepts (a-a_T) and
399 between the slopes (b-b_T) calculated by the least squares and by the Theil estimator. This
400 difference is disregarded for Eq. 3, because both a and b coefficients are not significant. The
401 greater discrepancies in the slopes occur in Eqs. 4 and 5, with about 7% of b while all the
402 others are < 1.5% of b. The low signification of intercepts in the simple linear regressions, plus
403 the small differences between b and b_T, allow one to discard the intercepts and to use slopes
404 calculated by Theil method. The results of the threshold EMv < EMh + 0.1 that produces for
405 the studied plot an increased number of inverted profiles (Table 5, Eqs. 4 and 5) advocate that
406 this technique merits further efforts.

407 The centrality and dispersion measures for the ECe estimations for the 250 sites within
408 the plot no. 2 can be compared with the same measures of the 40 ECe lab-determinations. The
409 means of the 40 lab determinations of ECe is 7.88 dS m^{-1} against 8.11 dS m^{-1} of the
410 estimations by Theil regression for the 250 reading sites, and the values of the medians are
411 6.38 dS m^{-1} against 7.21 dS m^{-1}, respectively. These differences are allowable for agricultural
412 purposes. The dispersion measures of the 40 lab determinations and the same measures of the
413 estimations for the 250 sites show a much great dispersion for the 40 lab measures. This
414 happens because the 40 sampling sites were not randomly selected, but were selected to cover
415 the full range of soil salinity appraised from our first EMI survey and field visits.

416 The low number of observations, a common circumstance for the small-sized fields of
417 Mediterranean agriculture, hampered the separate calibration for "regular" and "inverted"
418 profiles. The separate calibration, however, seems promising as shown by the results obtained
419 with the two assayed thresholds. This black-box approach encompasses the effects of the
420 saline water table and other soil features on the EMI signal, and can be easily tested when
421 further, similar paddies are studied. Other thresholds, either arbitrary or arising from new
422 designs of electromagnetic induction sensors, could be assayed for regrouping profiles for
423 separate adjustments with ECe.

The map resulting from the 40 ECe lab-determined values has to be compared with the map resulting from these values plus the estimations at the remaining 210 EMI sites using the Theil method (Fig. 8). Both maps in this Figure show the soil salinity classes relevant for agriculture (Soil Survey Division Staff 1993), with an overall agreement between the map without EMI data and that produced incorporating EMI data, and with the classical better detail furnished by the much greater number of sites with estimates obtained from EMI readings. A noticeable difference from this degree of detail is the more elongated shape and parallel disposition of the saline patches. This salinity pattern is attributed to the effect of past land cutting and levelling combined with the several non-fully functional parallel subsurface drainage pipes outlets to the drainage ditch. We deem the map of Fig. 8b as the most reliable.

Conclusions

The soil salinity of the targeted rootable horizon of a paddy with a densic pan underlayed by a supersaturated and saline layer can be mapped with a non-deterministic approach using electromagnetic induction. This approach did not need assumptions about the salinity distribution through the soil profile, or about the nature of the EM38 signal, or about the normality of the regressed variables. The readings of the EM38 sensor were calibrated with the soil salinity expressed as ECe of the targeted 40 cm depth. The similarity of the adjustments by the non-parametric Theil adjustment and by LSR agrees with previous results for nearby areas.

The rootable horizon of the studied paddy is strongly or very strongly saline (ECe $\geq$ 8 dS m^{-1}) in about a half the surface area. Only halophytes grow well in these conditions, and rice with running fresh water remains the only profitable crop. There is still lateral variability of soil salinity in spite of the long history of puddling and yearly inundation with running fresh irrigation water. However, the salinity of the upper soil layer of the studied plot is more homogeneous than in the nearby more recent paddies. The variability of soil salinity, not mirrored by the rice plants development, has been depicted with EMI measurements and a few soil samples.

453 The successful mapping for the upper 40 cm layer, in spite of the oversaturation by
454 saline water under the densic pan, proves that EMI is a powerful tool for further salinity
455 mapping in paddies. It will enable future studies to highlight the evolution of soil salinity with
456 a reduced number of soil samples. The main limitation for field surveying is paddy
457 trafficability, a condition that occurs only occasionally, and not in all paddies at the same time.

458 These kinds of maps will allow for future monitoring of soil salinity both for
459 environmental purposes and as a key soil feature to avoid fiascos when planting crops other
460 than rice.

461

462 **Acknowledgements.** Field and lab works were done at the Soils and Irrigation Unit, Zaragoza,
463 Spain. This article was funded by the Spanish Government (project AGL2012-40100) and by grant
464 FMI33/11 from Aragon, Spain. Thanks to Ms. Rosa Gómez for her help with the figures.

465

466 **REFERENCES**

467 Aimrun W, Amin MSM, Ezrin MH, Mastura M (2011) Paddy soil properties and yield
468 characteristics based on apparent electrical conductivity zone delineation for a humid
469 tropical rice farm. African J Agric Res 6: 5339-5350.

470 Aimrun W, Amin MSM, Ahmad D, Hanafi MM, Chan CS (2007) Spatial variability of bulk
471 soil electrical conductivity in a Malaysian paddy field: key to soil management. Paddy
472 Water Environ 5: 113-121.

473 Amezketa E (2006) An integrated methodology for assessing soil salinization, a pre-condition for
474 land desertification. J Arid Environ 67:594-606.

475 Chambers JM, Cleveland WS, Kleiner B, Tukey PA (1983) Graphical methods for data
476 analysis. Chapman and Hall, New York.

477 Daniel WW (1990) Applied nonparametric statistics, 2nd ed. Pws-Kent Publ Co. Boston, MA.

478 Díaz L, Herrero J (1992) Salinity estimates in irrigated soils using electromagnetic induction.
479 Soil Sci 154:151-157.

480 Enrique A, Bescansa P, Virto I (2005) Measuring salinity using electromagnetic sensors for
481 sustainable management of rice fields in the Ebro River Basin, NE Spain. Adv Geoecol
482 36: 559-567.

483 Ezrin MSM, Amin MSM, Anuar AR, Aimrun W (2010) Relationship between Rice Yield and
484 Apparent Electrical Conductivity of Paddy Soils. Am J Appl Sci 7: 63-70.

485 Glaister P (2005) A comparison of best fit lines for data with outliers. Internat. J. Math.
486 Education Sci Techn 36:110-117.

487 Herrero J (2008) Salinidad edáfica en varios salobrares de Aragón. Memorias de la Real
488 Sociedad Española de Historia Natural 4:1-164. Madrid, Spain. (In Spanish).

489 Herrero J, Pérez-Coveta O (2005) Soil salinity changes over 24 years in a Mediterranean
490 irrigated district. Geoderma 125:287-308.

491 Herrero J, Ba AA, Aragüés R (2003) Soil salinity and its distribution determined by soil
492 sampling and electromagnetic techniques. Soil Use Manage 19:119-126.

493 Herrero J, Netthisinghe A, Hudnall WH, Pérez-Coveta O (2011) Electromagnetic induction as
494 a basis for soil salinity monitoring within a Mediterranean irrigation district. J Hydrol
495 405:427-438.

496 Isaaks EH, Srivastava RM (1989) An introduction into applied geostatistics. Oxford
497 University Press, New York.

498 Islam MM, Cockx L, Meerschman E, De Smedt P, Meeuws F, Van Meirvenne M (2011) A
499 floating sensing system to evaluate soil and crop variability within flooded paddy rice
500 fields. Precis Agr 12: 850-859.

501 Lesch SM, Corwin DL, Robinson DA (2005) Apparent soil electrical conductivity mapping as
502 an agricultural management tool in arid zone soils. Comput Electron Agr 46:351-378.

503 Lesch SM, Rhoades JD, Lund LJ (1992) Mapping soil-salinity using electromagnetic
504 measurements. Soil Sci Soc Am J 56:540-548.

505 Li HY, Shi Z, Webster R, Triantafilis, J (2013) Mapping the three-dimensional variation of soil
506 salinity in a rice-paddy soil. Geoderma 195-196:31-41.

López-Bruna D, Herrero J (1996) El comportamiento del sensor electromagnético y su calibración frente a la salinidad edáfica. Agronomie 16:95-105. (In Spanish, with English summary).

McNeill JD (1980) Electromagnetic terrain conductivity measurement at low induction numbers. Technical Note 6. Geonics Ltd. Ontario, Canada (http://www.geonics.com)

Myers RH (1990) Classical and modern regression with applications. 2nd ed. Wadsworth Publishing Company. Belmont, CA.

Nogués J, Robinson DA, Herrero J (2006) Incorporating electromagnetic induction methods into regional soil salinity survey of irrigation districts. Soil Sci Soc Am J 70:2075-2085.

Nogués J, Herrero J, Rodríguez-Ochoa R, Boixadera J (2000) Land evaluation in a salt-affected irrigated district using an index of productive potential. Environ Manage 25:143-152.

Playán E, Pérez-Coveta O, Martínez-Cob A, Herrero J, García-Navarro P, Latorre B, Brufau P, Garcés J (2008) Overland water and salt flows in a set of rice paddies. Agr Water Manage 95:645-658.

Rhoades JD, Chanduvi F, Lesch SM (1999) Soil salinity assessment. Methods and interpretation of electrical conductivity measurements. FAO Irrigat Drainage Paper 57. FAO, Rome, Italy.

Soil Survey Staff (2010) Keys to Soil Taxonomy, 11th ed. Natural Resources Conservation Service, USDA. Washington, DC.

Soil Survey Division Staff (1993) Soil survey manual. Natural Resources Conservation Service, Handbook 18. USDA. Washington, DC.

United States Salinity Laboratory Staff (1954) Diagnosis and improvement of saline and alkali soils. Agriculture Handbook no. 60. USDA. Reprint 1969.

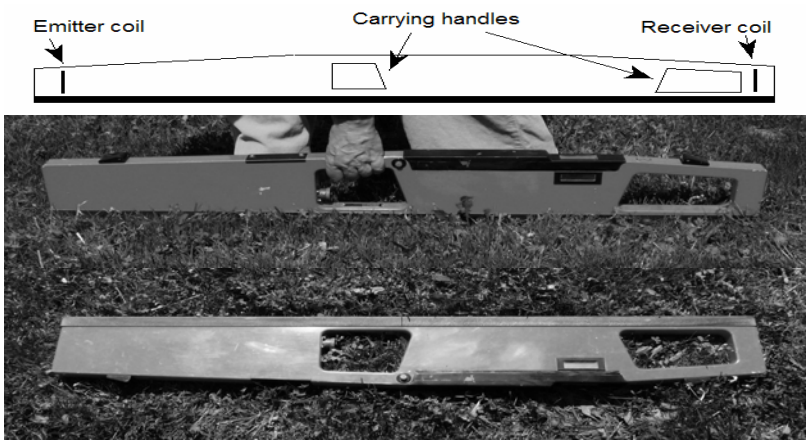

Fig. 1 Diagram of an EM38 sensor (a), the EM38 in vertical (b) and horizontal (c) position.

Fig. 2 Location of the Flumen irrigation district in the Ebro Valley, Spain

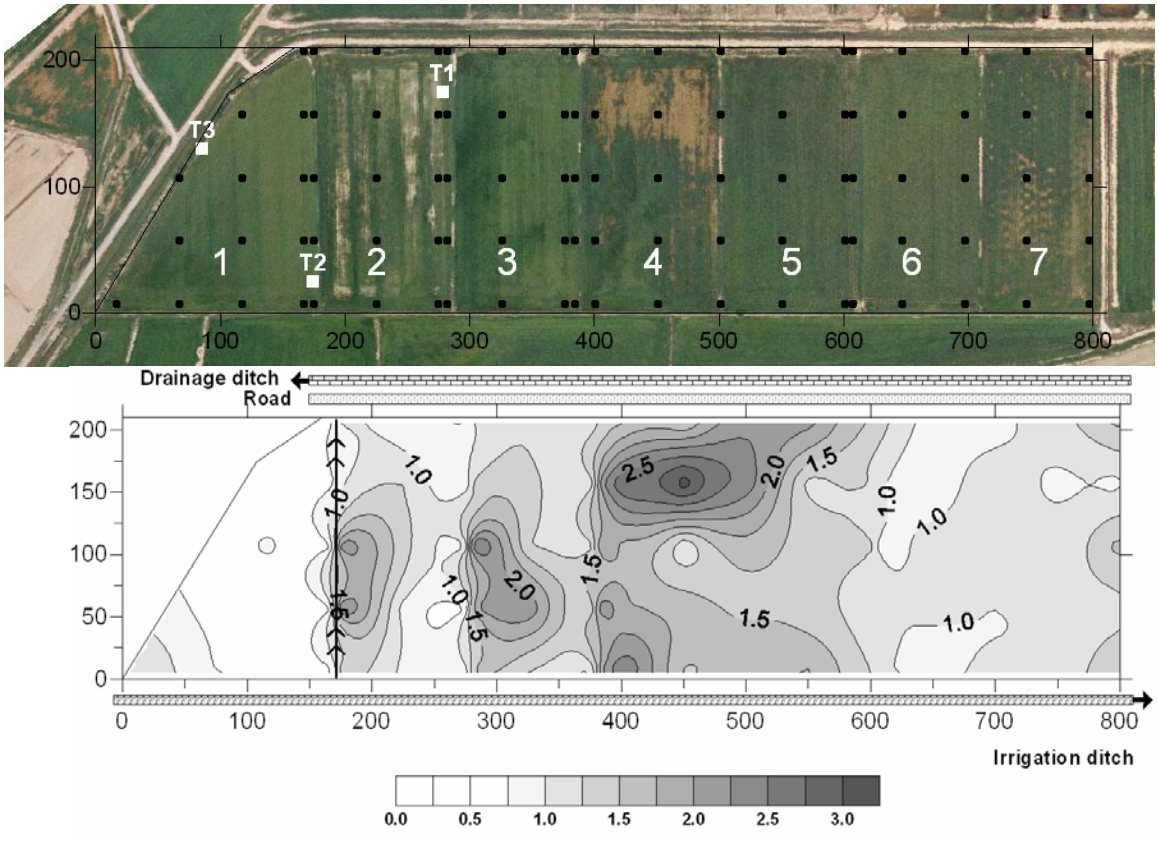

Fig. 3 The aerial image of the farm in 2006 shows the plot numbers and the observation wells (T1, T2, and T3) in white; black circles mark the EMI reading sites. The EMh map (axes in meters) of the entire farm was obtained from EM38 readings in September 10, 1999. Arrows on the ditches and the pipe drain show the water flow direction.

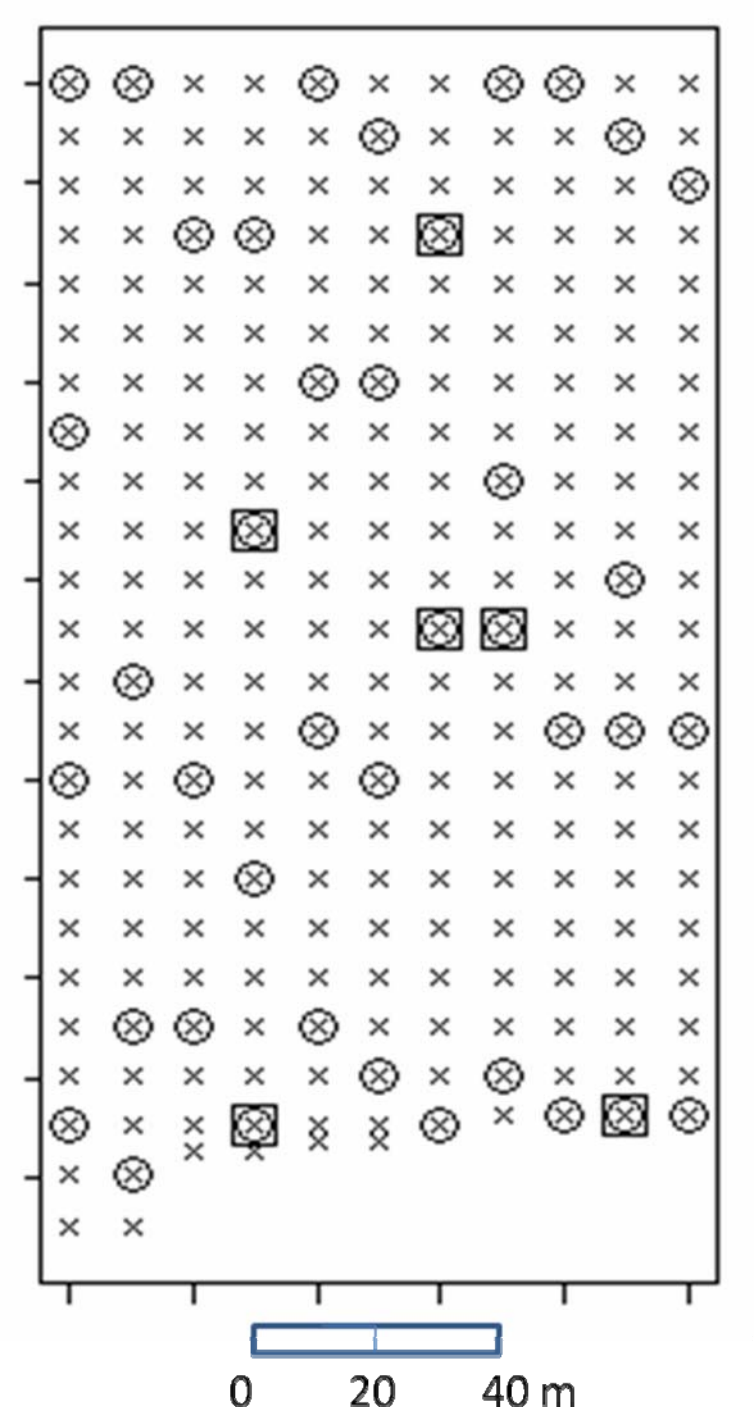

Fig. 4 Distribution of the 250 EMI readings (crosses) within the plot no. 2. Soil samples were also taken at 40 of these sites, marked with circles, for θ, PS, and ECe determination. Other chemical analyses (Table 2) were performed on the samples from the sites marked with squares.

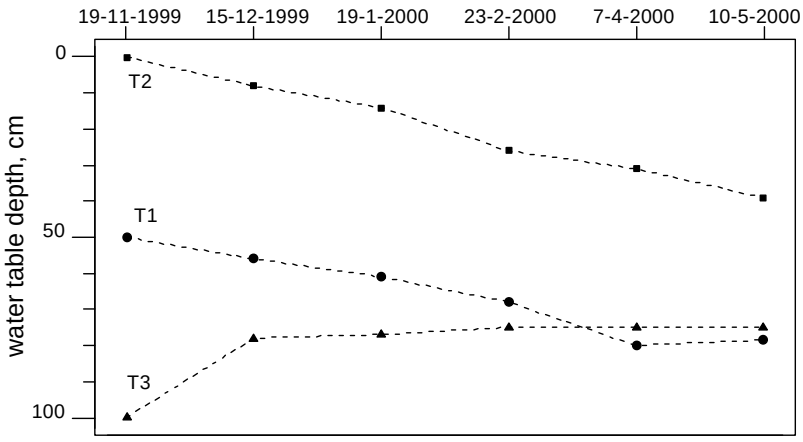

Fig. 5 Water table depth at six dates in the three observation pipes T1, T2, and T3.

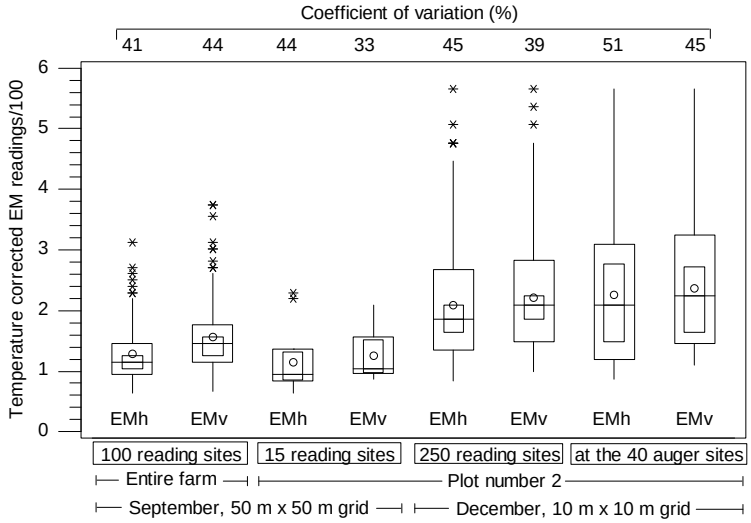

Fig. 6 Boxplots of EMh and EMv (i) at the 100 reading sites in the entire farm with 50 m ×50 m orthogonal grid, (ii) at 15 of these sites falling within plot no. 2, (iii) at the 250 reading sites within plot no. 2, and (iv) at the 40 of those sites where soil cores were taken immediately after the EMI readings.

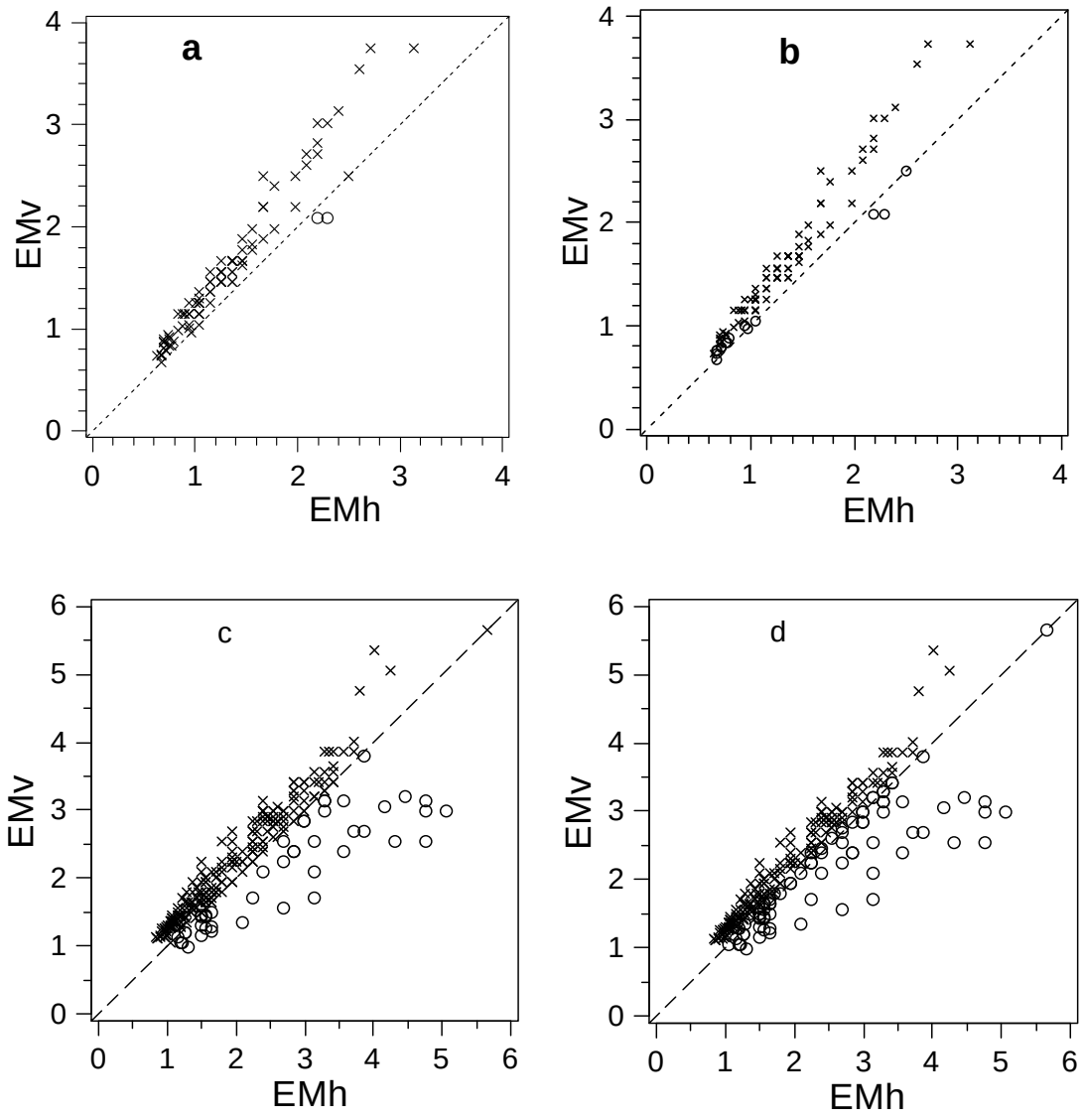

Fig. 7 EMh and EMv at the 100 reading sites in the farm (a and b), and at the 250 reading sites in the studied plot (c and d). Crosses at the graphs a and c are for those sites where EMv ≥ EMh; crosses at the graphs b and d are for sites where EMv ≥ EMh + 0.1. Circles are for sites with EMv below the mentioned thresholds. Dashed line is EMv = EMh.

577

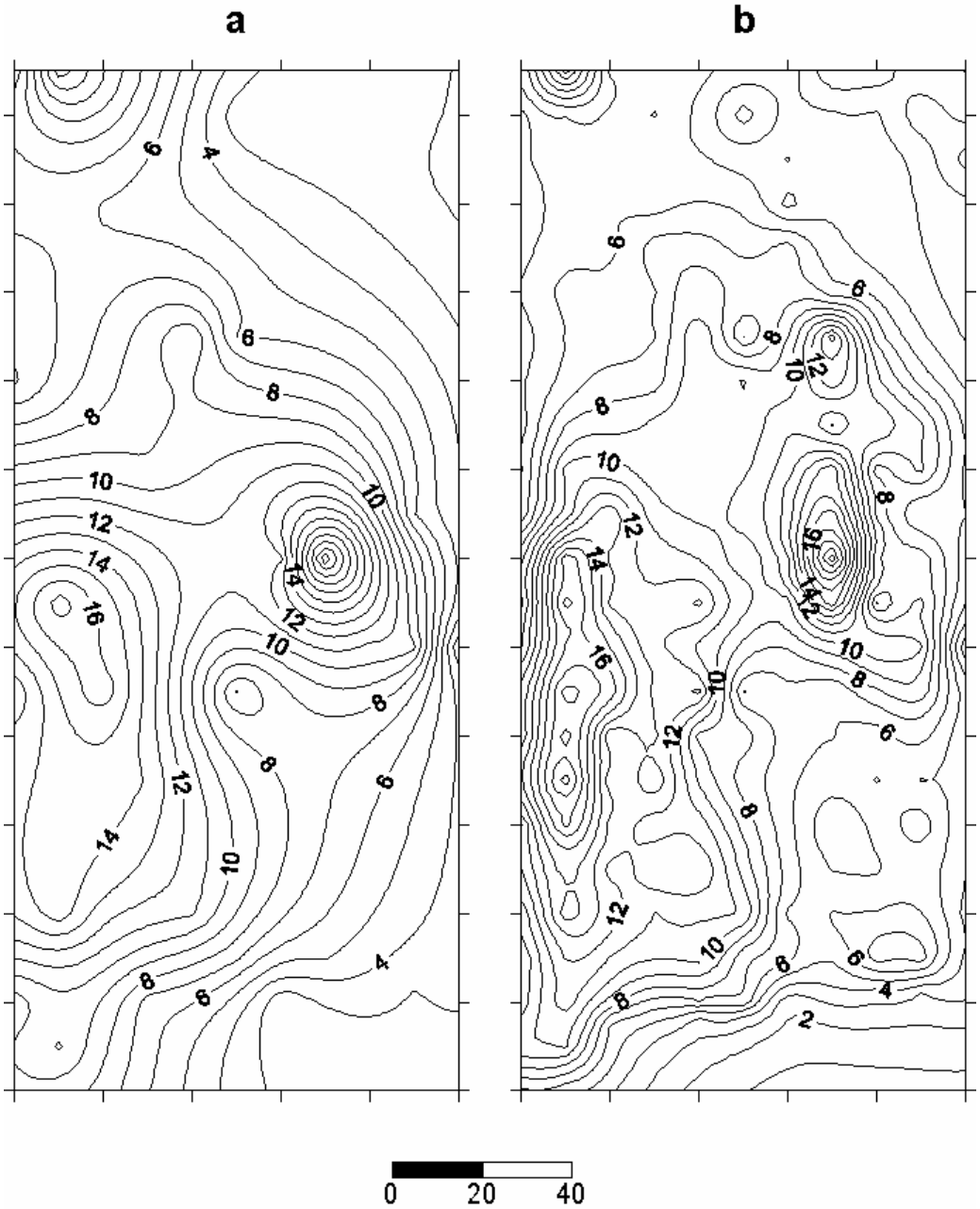

578

579 **Fig. 8** Contour lines of ECe (dS m^{-1}) obtained from the lab determinations at the 40
580 augered sites (Map a), and from the same data plus the estimates at the remaining 210 sites
581 with Theil slope estimator (Map b). Bar scale is in meters.

582

Table 1 Analytical results for the soil profile at plot no. 1.

Samples taken in 1979, before conversion in a paddy										
Horizon	Depth cm	OM %	pH 1:2.5	CCE %	PS %	ECe dS m^{-1}	Ca^{2+}	Mg^{2+}	Na^{+}	SAR $(meq\ L^{-1})^{0.5}$
							meq L^{-1}			
Ap	0-7	1.20	9.10	22	60.0	99.83	36.0	74.0	1391.3	188
BA	7-43	0.66	8.94	23	58.0	36.25	30.5	24.0	380.4	73
B2	43-84	0.38	9.05	26	60.5	32.71	29.0	23.5	391.3	76
C	84-110	0.13	9.13	27	42.0	35.58	28.8	22.8	434.8	86
Cy	110-120	0.26	9.02	27	58.0	37.13	29.5	25.0	460.9	88
Cy	138-145	0.25	8.99	23	62.0	37.45	32.2	16.7	469.6	95

OM = organic matter; CCE = calcium carbonate equivalent; PS = percent saturation; ECe = electrical conductivity of the saturation extract; SAR = sodium adsorption ratio.

Average ECe (dS m^{-1}) for consecutive soil layers						
Depth, cm	0-20	20-40	40-60	60-80	80-100	100-120
1979-1980	50.54	37.01	31.01	29.34	33.17	26.40
1999-2000	3.15	1.67	1.08	1.18	1.42	1.87

Table 2 Observations performed on the studied farm in 1999.

Date	Surface extent, ha	EM38 readings			Soil samples	
		Grid, m × m	horizontal dipole	vertical dipole	Number	Depth, cm
10 September	14	50 × 50	100	100	0	-
15 December	2	10 × 10	250	250	40	0-40

Table 3 Analytical results for six of the 40 soil samples taken on December 15, 1999 from the surface layer (0-40 cm) of the studied plot no 2.

ECe	PS	pHe	Ca^{2+}	Mg^{2+}	Na^{+}	HCO_3^{-}	Cl^{-}	SO_4^{2-}	SAR
dS m^{-1}	%		meq L^{-1}						$(meq\ L^{-1})^{0.5}$
2.96	42	8.18	15.7	6.8	10.8	2.6	7.4	24.5	3.23
3.63	51	8.13	11.3	10.4	20.6	2.4	9.9	31.8	6.26
9.13	62	7.95	19.0	22.1	70.6	1.8	42.2	79.6	15.59
11.75	61	8.02	12.7	30.4	105.0	2.2	57.7	96.3	22.62
16.60	58	7.92	23.7	40.9	158.5	2.0	92.9	140.2	27.90
20.80	56	7.97	16.7	44.0	223.7	1.4	110.8	182.9	40.58

Table 4 Regression equations (EMv = $a + b \times$ EMh), number of computed sites (n) and percent of the total number of observations (% n), coefficient of determination (r^2), and standard error (SE) in dS m^{-1}. Two different criteria (EMv ≥ EMh, and EMv ≥ EMh + 0.1) were assayed for assigning sites to the class "high contribution of deep soil to EMI readings".

Computed	n	%n	*a*	*b*	r^2	SE
	The entire farm; September 10, 1999					
All readings	100		-0.058 (0.190)	1.250	0.94	0.17
EMv ≥ EMh	98	98	-0.107 (0.005)	1.299	0.96	0.14
EMv < EMh	2	2				
EMv ≥ EMh + 0.1	85	85	-0.113 (0.004)	1.316	0.97	0.12
EMv < EMh + 0.1	15	15	0.131	0.902	0.99	0.05
	The studied plot; December 15, 1999					
All readings	250		0.544	0.798	0.76	0.42
EMv ≥ EMh	206	82	0.213	1.033	0.95	0.19
EMv < EMh	44	18	0.496 (0.002)	0.593	0.77	0.38
EMv ≥ EMh + 0.1	170	68	0.180	1.079	0.97	0.16
EMv < EMh + 0.1	80	32	0.503	0.673	0.74	0.43
	Only the augered sites; December 15, 1999					
All readings	40		0.465 (0.004)	0.839	0.84	0.44
EMv ≥ EMh	36	90	0.242 (0.001)	0.988	0.98	0.17
EMv < EMh	4	10	0.776 (0.123)	0.416 (0.046)	0.91	0.27
EMv ≥ EMh + 0.1	26	65	0.195 (0.002)	1.050	0.99	0.13
EMv < EMh + 0.1	14	35	0.441 (0.274)	0.753	0.75	0.59

Significance levels of *a* and *b* are indicated in parenthesis whenever > 0.0001.

Table 5 Ordinary least squares regression equations (ECe = $a + b \times$ EM) of ECe on EMh and EMv, with the number of computed sites (n), coefficient of determination (r^2), and standard error (SE), followed by the differences with the Theil's estimation of intercept (a-a_T) and slope (b-b_T).

Eq. #	Independent variable	n	*a*	*b*	r^2	SE dS m^{-1}	a-a_T	b-b_T
1	EMh	40	-0.726 (0.266)	3.816	0.86	1.84	0.451	-0.055
2	EMh (only EMv ≥ EMh)	36	-1.154 (0.046)	3.903	0.90	1.48	0.110	0.042
3	EMh (only EMv < EMh)	4	4.580 (0.345)	2.716 (0.143)	0.74	3.41	3.384	-0.703
4	EMh (only EMv ≥ EMh + 0.1)	26	-1.070 (0.127)	3.774	0.86	1.51	0.003	0.226
5	EMh (only EMv < EMh + 0.1)	14	1.091 (0.457)	3.448	0.82	2.19	1.244	-0.259
6	EMv	40	-0.682 (0.541)	3.631	0.65.	2.85	1.007	0.017

Significance levels of *a* and *b* are indicated in parenthesis whenever > 0.0001.